DE GRUYTER
OPEN

Arch. Min. Sci., Vol. 61 (2016), No 1, p. 137–156

Electronic version (in color) of this paper is available: http://mining.archives.pl

DOI 10.1515/amsc-2016-0011

GANG WANG*,**,***, WANPENG HUANG**,[1], LULU SUN**, MENGMENG WU**, XIAOQIANG ZHANG**

HIGH DRILLING METHANE DRAINAGE IN FRACTURING ZONES FORMED BY WATER INJECTION INTO BOREHOLES

ODPROWADZANIA METANU METODĄ ODWIERTÓW DOKONYWANYCH W STREFIE SZCZELIN POWSTAŁYCH WSKUTEK WPROWADZANIA WODY DO OTWORÓW

Methane drainage method should be used before coal mining of many modern collieries because ventilation air methane is insufficient to keep methane level within regulation values. The technology of high drilling methane drainage (HDMD) has been used for methane drainage although its effect is not very stable due to parameter design. The height of the fracturing zones is determined mostly according to empirical formula, on-site observation and numerical simulation analysis. In this paper, a method was introduced for determining the height of the air fracturing zones (AFZs) based on its high similarity to the characteristics of Fracturing zones and the relationship between the height of Fracturing zones and the strain of overlying rock strata. The application of water injection in both Shuangdingshan and Dongrong collieries found that the theoretically calculated the height of the Fracturing zones was approximately equal to the measured one in field tests within a permissible error of less than 5%, proving that the method is feasible. Based on the designed drainage parameters, the utilization of HDMD technology in the collieries mentioned above found that the methane concentrations in both tail gate and upper corner were controlled in the ranges of 0.17% to 0.32% and 0.26% to 0.84%, respectively. These results showed that the water injection verified HDMD in Fracturing zones could effectively solve the problem of methane overrun and also verified the accuracy and reliability of its related theory.

Keywords: high drilling, methane drainage, water injection, fracturing zones, strain

Przed rozpoczęciem wydobycia węgla w wielu obecnie eksploatowanych kopalniach wskazane jest odprowadzenie metanu, ponieważ stosowane systemy wentylacji powietrza są niewystarczające aby utrzymać stężenia metanu na dopuszczalnym poziomie. Technologia odprowadzania metanu metodą odwiertów prowadzonych na różnej wysokości (HDMD) wykorzystywana jest w tym celu, choć jej wyniki

* STATE KEY LABORATORY OF COAL MINE DISASTER DYNAMICS AND CONTROL, CHONGQING UNIVERSITY, CHONGQING, 400030
** SHANDONG UNIVERSITY OF SCIENCE AND TECHNOLOGY, COLLEGE OF MINING AND SAFETY ENGINEERING, SHANDONG QINGDAO, 266590
*** CHINA COAL TECHNOLOGY ENGINEERING GROUP CHONGQING RESEARCH INSTITUTE, CHONGQING, 400037
[1] CORRESPONDING AUTHOR, E-MAIL: huangwanpeng2002@126.com

nie zawsze są stabilne ze względu na konieczność doboru parametrów obliczeniowych. Wysokość strefy szczelinowania określa się zazwyczaj empirycznie, na podstawie obserwacji w terenie oraz drogą symulacji numerycznych. W pracy tej określono wysokość strefy wykonania szczelin w oparciu o podobieństwo do charakterystyk *Strefy szczelinowania* oraz o analizę odkształceń warstw nadkładu. Zastosowano wtrysk wody w kopalniach Shuangdingshan i Dongrong i stwierdzono, że teoretycznie obliczona wysokość stref szczelinowania była w przybliżeniu równa wysokości zmierzonej empirycznie w trakcie badań terenowych, z dopuszczalnym poziomem błędu poniżej 5%, co wskazuje na możliwość zastosowania metody. W oparciu o parametry obliczeniowe stwierdzono, że zastosowanie metody HDMD w wyżej wymienionych kopalniach spowodowało, że stężenia metanu rejestrowane w chodniku nadścianowym i górnych narożach utrzymywały się odpowiednio na poziomie 0.17%, 0.32% i 0.26%-0.84%. Wyniki te pokazują, że wtrysk wody w strefie szczelin pomaga skutecznie rozwiązać problem obecności zbyt wysokich ilości metanu, ponadto potwierdza dokładność i wiarygodność teorii na której metoda jest oparta.

Słowa kluczowe: odwierty, odprowadzenie metanu, wtrysk wody, szczelinowanie, odkształcenia

1. Introduction

Coal methane is one of the major disaster factors in coal mining. Its outburst may result in a large number of casualties and economic losses (Flores, 1998; Wang et al., 2014). Methane drainage and ventilation air methane are the most important solutions to gas outbursts (Noack, 1998). In recent years, with the mining depth and strength increasing, the permeability of coal seams becomes smaller, while the methane content and the methane emissions obviously increase. Under this circumstance, ventilation air methane and protective coal seam exploitation aren't enough to keep methane level within the regulation values (Liu et al., 2009). Methane drainage as the most effective means has been widely used in China (Wang et al., 2012; Frank et al., 2013; Lu et al., 2009).

Since an earliest underground coalbed methane drainage test in China was conducted at Fushun colliery, Liaoning Province (Sang et al., 2010; Li et al., 2014), methane drainage has been widely used in China. HDMD has greater flexibility in selecting drainage layers in addition to a big drainage capacity, simple process and small drainable quantity. Due to its parameter design and other factors (Zhai et al., 2013; Liu et al., 2011; Peng et al., 2012), its drainage effect is not very stable and satisfactory. In the actual drainage, how to determine the high level of air fracturing zones is unclear yet.

Because the air fracturing zones (AFZs) and the fracturing zones are similar in their characteristics, air can flow from the lower to the upper fracturing zones. Therefore, high level of AFZs can be found through Fracturing zones (Zhang et al., 2012). Currently, the height of Fracturing zones are obtained through field test and theoretical calculations using empirical formula (Miao et al., 2011; Goran et al., 2014), similar material simulation (Dai et al., 2010; Ren et al., 2010; Castro et al., 2007), numerical analysis (Chen et al., 2012; Xu et al., 2010), petrophysical logs (Tokhmchi et al., 2010; Perez et al., 2013), etc. The field test is the main method and includes water injection methods, resistivity methods, micro-seismic methods, acoustic methods, TV imaging methods, and microfocus X-ray computed tomography methods, etc. Singh and Kendorski (1983) have found that there are three zones (caved zone, fracture zone and continuous deformation zone) of disturbance in the overburden strata in response to mining. Abbas et al. (2012) proposed that the height of destressed zone is taken as equivalent to the combined height of the caving and fracturing zones above the mined panel roof. The relationship between the height of Fracturing zones and the strain of overlying rock strata has not been well investigated.

In order to guide methane drainage, this paper deals with the relationship between the height of Fracturing zones and the strain of overlying rock strata. This relationship was justified by the water injection in Dongrong colliery and Shuangdingshan colliery, Shandong and Jilin Province, China. According to the formula of the strain, methane drainage was applied at the 7433 coal face of Kongzhuang colliery, Jiangsu Province, China.

2. Theoretical analysis

Because of the overlying rock strata subsidence, it suffers bent deformation and rock undergoes stretch. When the rock reaches its tensile strength, the perpendicular fracture will be produced and fault fissures might be formed if it continues to develop. Therefore, the rock bending deformation is the main reason for the formation of Fracturing zones (Wang et al., 2014), as shown in Fig. 1.

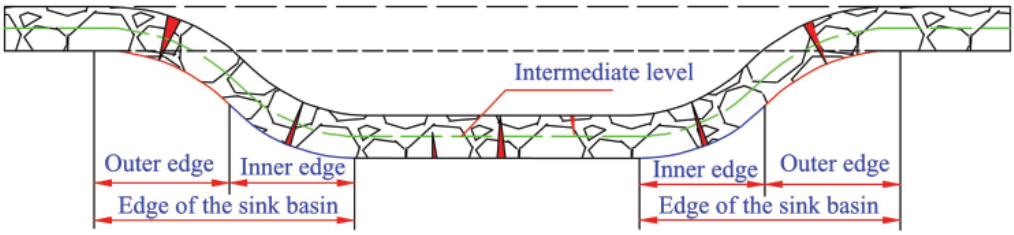

Fig. 1. Sketch map of rock stratum's tensile deformation

Assuming that there are two segments of arcs that well match the inner and outer edges of the rock basin subsidence curves and have equal curvatures and arc lengths and opposite curvature directions, thus, 1) the inflection point of the settlement curve is the connecting point of the two arcs at which the curvature is zero and two arcs connect smoothly; and 2) according to the maximum subsidence and displacement angle, the rock's tensile deformation can be worked out by calculating the length of the arc segment. The formulas for calculation are very simple and the results are accurate.

2.1. Model and formula for calculating strain

Tensile deformation of the intermediate layer rock is characterized by the size and distribution of fractures and the strain of the intermediate layer rock can be used to represent rock deformation. As shown in Fig. 2, the strain (ε) is defined as the ratio of the increment of the length to the original length, i.e.

$$\varepsilon = (l_1 - l_0)/l_0 \tag{1}$$

where l_1 is the length of the arc of the intermediate layer rock subject to bending deformation, m; and l_0 is the length of the straight line segment of the intermediate layer rock without bent deformation, m.

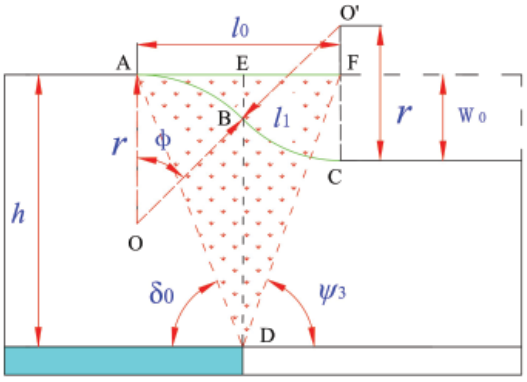

Fig. 2. Geometrical model for calculating rock stratum bending and subsidence

According to the geometric relations shown in Fig. 2, $l_0 = AE + EF$, $AE = h \cdot \cot\delta_0$, $EF = h \cdot \cot\psi_3$, the straight line segment length is found to be

$$l_0 = h \cdot (\cot\delta_0 + \cot\psi_3) \tag{2}$$

where h is the vertical distance from the roof of a coal seam to the intermediate layer rock, m; δ_0 is the angle of subsidence, (°); and ψ_3 is the full mining angle.

Assuming that δ_0 and ψ_3 are comparable to each other, thus,

$$\psi' = \delta_0' = (\psi_3 + \delta_0)/2.$$

According to Fig. 2, the length of arc of the intermediate layer rock subject to bending deformation is found to be

$$l_1 = 2r \cdot \phi \cdot \pi/180 \tag{3}$$

where r is the radius, m; and ϕ is the arc angle, (°).

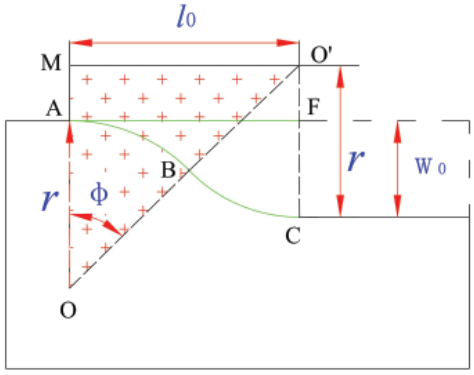

Fig. 3. Geometrical relationship of the model

For the $\Delta OO'M$ shown in Fig. 3, there are following geometrical relations:

$$OO'^2 = OM^2 + MO'^2,\ OO' = 2r,\ MO' = l_0,$$

$$OM = OA + AM = OA + FO' = OA + (CO' - CF) = r + (r - w_0),$$

$$(2r)^2 = \left(r + (r - w_0)\right)^2 + l_0^2,\quad \phi = \arcsin\frac{l_0}{2r}$$

Combining them find:

$$r = \frac{w_0^2 + l_0^2}{4w_0},\ \phi = \arcsin\frac{2w_0 \cdot l_0}{w_0^2 + l_0^2} \tag{4}$$

where w_0 is the maximum distance rock subsidence, m; $w_0 = m \cdot q$ where m is the thickness of mining coal seam, m; and q is the coefficient of rock subsidence. Generally, the coefficient (q) in the Fracturing zones is greater than the coefficient of surface subsidence (q_0). Because of the coefficient of the roof rocks of a coal seam subsidence ($q = 1$), the coefficient of rock subsidence at the height h can be found to be

$$q = 1 - (1 - q_0)h/H \tag{5}$$

where h is the vertical distance from the roof of coal seam to the intermediate layer rock, m; and H is the depth of the coal seam, m.

The steps to calculate the strain of the intermediate layer rock (ε), are as follows:

1) Calculate the subsidence coefficient q: $q = 1 - (1 - q_0)h/H$;
2) Calculate w_0 and l_0: $\begin{cases} w_0 = m \cdot q \\ l_0 = h \cdot (\cot\delta_0 + \cot\psi_3) \end{cases}$;
3) Calculate ϕ and l_1: $\begin{cases} \phi = \arcsin\left[2w_0 \cdot l_0 / (w_0^2 + l_0^2)\right] \\ l_1 = (w_0^2 + l_0^2) \cdot \phi \cdot \pi / (180 \cdot 2w_0) \end{cases}$;
4) Calculate ε: $\varepsilon = (l_1 - l_0)/l_0$.

2.2. Determination of Fracturing zones height

The ratio of the height of the Fracturing zones to the thickness of mining coal seam is called as k (H-T ratio), the top of rock in the Fracturing zones is characterized by the critical strain (ε_0), as shown in Fig. 4.

The height of the Fracturing zones is directly related to the uniaxial tensile strength. According to the correlation between rock parameters, the uniaxial tensile strength is proportional to the uniaxial compressive strength, and the relationship between the height of the Fracturing zones and the rock lithology is studied using strength coefficient (f). Therefore, the height of the Fracturing zones can be obtained based on the relationships of k as well as ε to f.

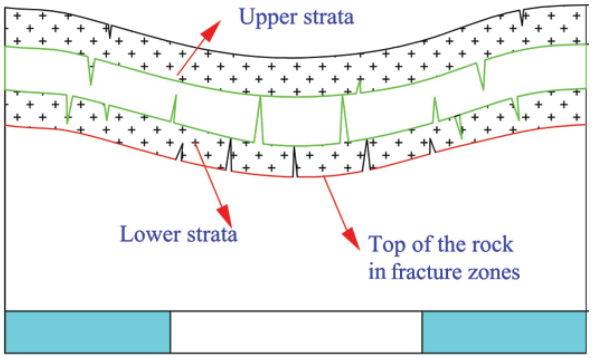

Fig. 4. Location relationship of rock strata within Fracture zones

With the colliery worker helps, the statistical results of field observation of the Fracturing zones height were obtained, the rock strata samples originate from underground mines of different locations of China. The strain of the lower, upper and intermediate layer rock were calculated and shown in Table 1. It can be seen from Table 1 that the *k* ratio is 7.8~8.3, 10.0~15.88, and 19.2 for soft and weak, medium hard and hard and strong rocks, respectively, and the critical strain is >0.40%, 0.1%~0.24% and 0.04% for soft and weak, medium hard and hard and strong rocks, respectively.

TABLE 1

Relationships of strain and *k* ratio to rock type

Colliery	Mining thickness /m	The height of the Fracturing zones /m	*k*	Rock type	Strength coefficient (*f*) in fracture zone	Rock strain ε/%		
						Lower strata	Top of the rock critical elongation	Upper strata
Linnancang	4.26	33	7.75	Weak	1.5	0.48	0.43	0.34
Longdong	4.3	34	7.9	Weak	1.5	0.55	0.47	0.41
Beizao	3.6	30	8.3	Weak	1.3	0.52	0.40	0.33
Hedong	3.6	36	10.0	Medium-hard	3.0	0.28	0.24	0.23
Yaoqiao	4.9	63.6	13.0	Medium-hard	3.5	0.18	0.13	0.11
Qianjiaying	3.0	40	13.3	Medium-hard	3.4	0.14	0.14	0.08
Cuizhuang	2.0	27	13.5	Medium-hard	3.3	0.22	0.13	0.11
Xinglong	2.8	41	14.6	Medium-hard	4.0	0.16	0.11	0.09
Shenjiazhuang	4.16	63.6	15.3	Medium-hard	4.5	0.14	0.11	0.09
Tangshan	10.14	161	15.88	Medium-hard	4.4	0.11	0.10	0.09
Tielin	1.7	32.7	19.24	Hard	5.5	0.05	0.04	0.03

Fig. 5 as shows the relationship between the *k* ratio and *f*. It is obvious that their relation is linear and can be formulated as Eq. (6) by the regression analysis method. It is clear from the formula that the harder the rock is, the greater the *k* ratio will be.

$$k = 2.63f + 4.47 \tag{6}$$

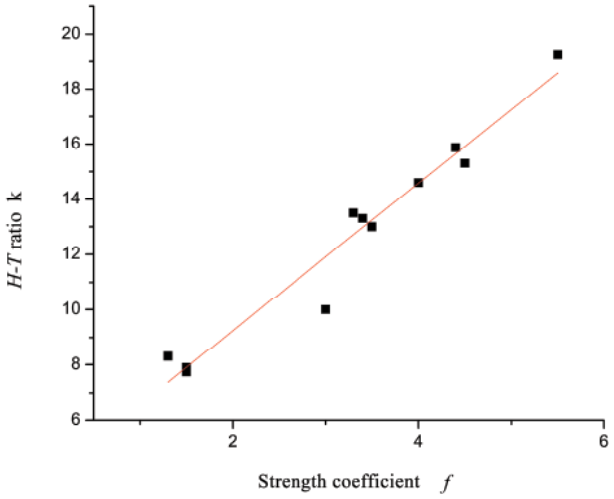

Fig. 5. Relationship between k ratio and f

3. Theoretical tests

3.1. Observation of Fracturing zones height by water injection

3.1.1. Observation mechanism

To observe the Fracturing zones height, the upward-inclined boreholes around the coal face are drilled through the Fracturing zones overlying the goaf by using the double-head water-stop machine drilling technology (Zhang et al., 2012; Cheng et al., 2015), as shown in Fig. 6.

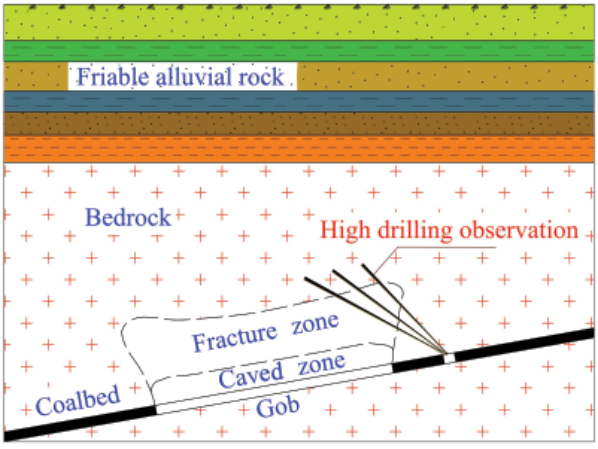

Fig. 6. Observation of Fracturing zones height by upward-inclined boreholes

3.1.2. Observation system

The observation system consists of three parts: double-head water-stop machine, two connecting tubes, one of which is expansion tube and the other is water injection tube, and two consoles, one of which is the expansion console and the other is the water injection console, as shown in Fig. 7. The double-head water-stop machine consists of two expansion capsules and probe water injection, as shown in Fig. 8. The expansion console and expansion tubes are connected, respectively, with two capsules of the double-head water-stopped machine and constitute a control system for controlling the expansion and contraction of the capsule. The water injection console and the water injection tubes are connected with the probe water injection of the double-head water-stop machine and constitute the observing device of this observation system.

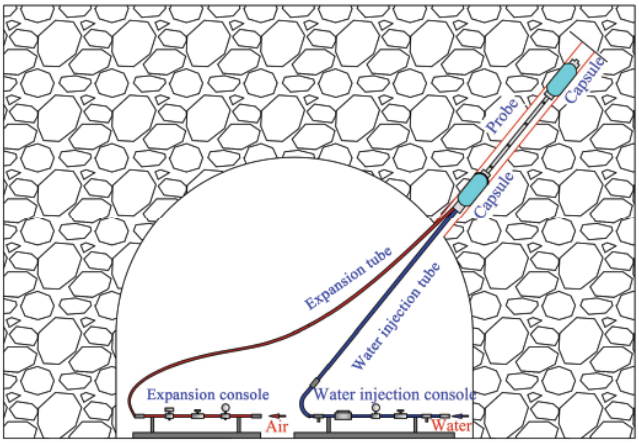

Fig. 7. Sketch map of the height of the Fracturing zones observation by upward-inclined boreholes

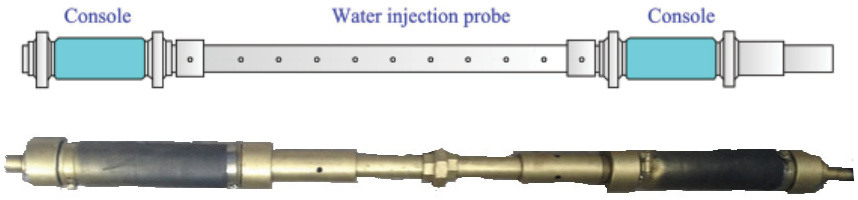

Fig. 8. Structure of double-head water-stop machine

3.1.3. Observation method

The steps for observing the Fracturing zones height are as follows:

1) Drill upward-inclined boreholes through the Fracturing zones. In the proper positions of the surrounding working face, upward-inclined boreholes are drilled from the Fracturing zones overlying the goaf through the Fracturing zones into the bend at a certain distance, usually 5 to 10 m.

2) Use the probes double-head water-stop machine to test the rock permeability. Use the observing device to measure the rock permeability from the top to the bottom of the borehole at intervals of 1 m. The maximum height of the permeable rock measured on-site is the Fracturing zones height.
3) The double-head water-stop machine manipulation and permeable rock observation. The steps for observing a high level rock permeability are as follows: (1) Operate the expansion console to make sure the two capsules in a free state; (2) Adjust the double-head water-stop machine to get into place by using drill rig; (3) Operate the expansion console to make sure the capsule is in a pressure expansion state and plug the holes in the period of drilling; (4) Use the flowmeter to observe its seepage quantity per unit of time by operating the water injection console and measure its permeability.

3.2. Field application in Dongrong colliery

3.2.1. Scheme design

Water injection method was applied in the right 16-th coal face at Dongrong colliery in China. The thickness of the mining coal seam was 2.0 m. The height of the Fracturing zones is expected to have upper limit of $H_u = 16 \cdot M = 16 \times 2.0 = 32$ (m), lower limit of $H_l = 12 \cdot M = 12 \times 2.0 = 24$ (m) and the caved zone height of $H_c = 5 \cdot M = 5 \times 2.0 = 10.0$ (m). The boreholes for observation were drilled from drainage roadway to the right of the 16-th coal face. Table 2 lists their related data, and Fig. 9 shows the cross-sectional view of the borehole layout in the right 16-th coal face.

TABLE 2

Data of boreholes in the right 16-th coal face

Hole No.	Dip angle	Length (m)	Aperture (mm)
I	50°	65	ϕ89
II	55°	60	ϕ89

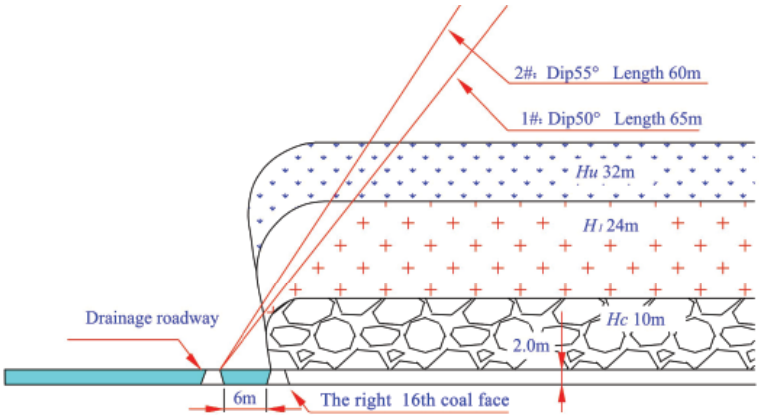

Fig. 9. Cross-sectional view of boreholes layout in the right 16-th coal face

3.2.2. Results and analysis

According to the measured data, the seepage quantity and water outflow of 1# and 2# drilling were shown in Fig. 10.

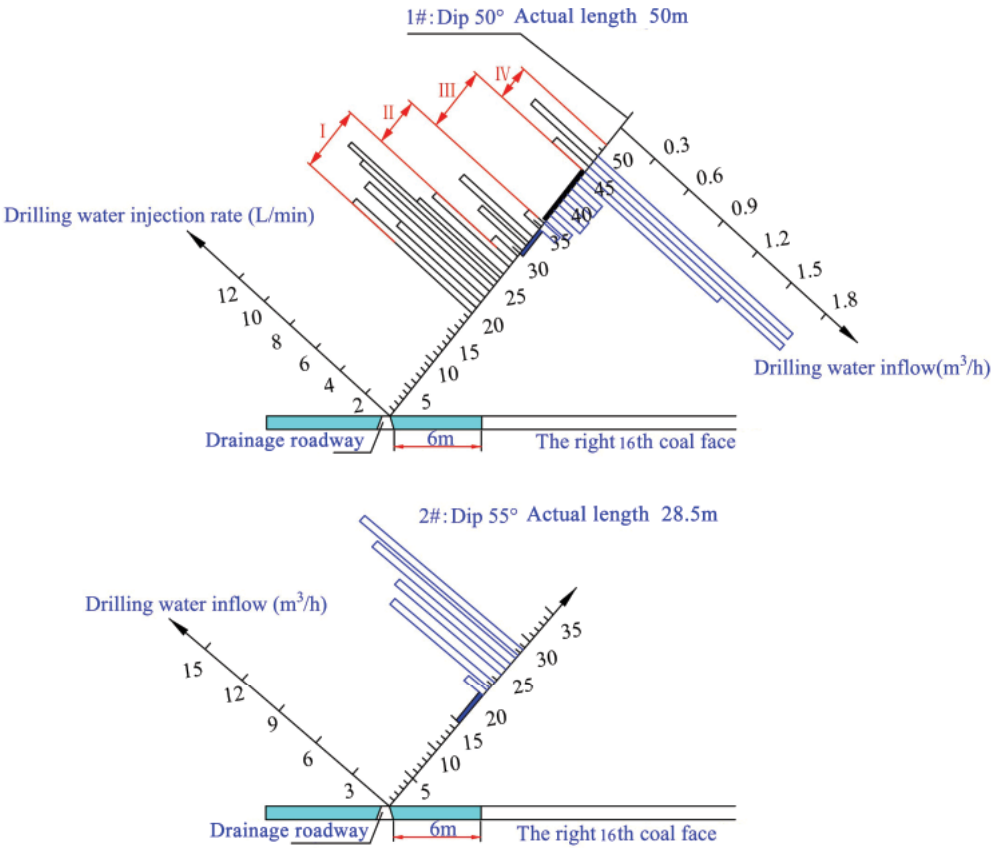

Fig. 10. Observed results of 1# and 2# drillings

1) Observation of 1# drilling

From Fig. 10, the boreholes in the IV drilling area were 45.75~50 m long and 35~38.3 m high and located on the top of the aquifer, which was less affected by mining and had no developed secondary cracks. Its seepage quantity was from 2.7 to 5.0 L/min.

The boreholes in the III drilling area were 36.75~44.25 m long and 28.1~33.9 m high and located in the aquifer. When the probe capsules were closed, its water outflow reduced from 1.69 m^3/h to 0.13 m^3/h. As the Fracturing zones was not cross to the aquifer, the upper limit of its height of the Fracturing zones was smaller than or equal to 28.1 m.

The boreholes in the II drilling area were 29.25~35.25 m long and 22.4~27 m long. The seepage quantity in the area was from 1.2 to 5.3 L/min, basically equal to that in the IV drilling area. Therefore, secondary cracks were not developed, showing no Fracturing zones in this area.

The boreholes in the I drilling area was 19.5~27.75 m long and 14.9~21.3 m high. The seepage quantity in the area was from 6.1 to 11.8 L/min and greater than 9 L/min for most of rocks. So these drillings penetrated the Fracturing zones and the maximum height of the Fracturing zones was from 21.3 to 22.4 m.

2) Observation of 2# drilling

When the upward-inclined boreholes were 22.5 m long and 18.45 m high, water outflow increased from 1.5 to 7.9 m^3/h. When the upward-inclined boreholes were 22.5 m long and 23.37 m high, water outflow was the maximum, reaching 13.32 m^3/h. At this point the drilling had completely moved into the aquifer. Due to higher water outflow, the drilling was stopped. After three days observation, water outflow was stabilized at 8.5 m^3 /h.

Overall, because of high water outflow, the height of the Fracturing zones didn't reach the height of the aquifer. Therefore, the measured Fracturing zones height was less than 18.45 m.

3.2.3. Determination of Fracturing zones height

Table 3 lists data related to rock strata. From Table 3, it can be seen that from the 16-th coal face to coarse sandstone of 1.0 m thickness, the vertical height was 21.3 m, consistent with 1# observational data. The vertical height from coal place to fine sandstone was 21.3 m, beyond the scope of field measurements. To ensure safe production, the maximum observed result would be the height of the Fracturing zones in the right 16-th coal face. Combined the characteristics of geology with the observed results of seepage quantity, the height of the Fracturing zones in the right 16-th was 21.3 m. Table 4 shows the measured and theoretical data of Dongrong colliery.

TABLE 3

Data of geological drilling in Dongrong colliery

Lithology	Thickness /m	Cumulative thickness /m	Vertical height from coal face /m
Siltstone	0.65	30.6	28.85
Fine sandstone	6.9	37.5	28.2
Coarse sandstone	1.0	38.5	21.3
Siltstone	0.8	39.3	20.3
…	…	…	…
16-th Coal	2	60.8	0

TABLE 4

Comparison between measured the height of the Fracturing zones and theoretically calculated value

Colliery	Mining thickness /m	Rock type	Strength coefficient (f) in fracture zone	The measured height of the Fracturing zones /m	The theoretical height of the Fracturing zones /m	Error
Dongrong	2.0	Medium-hard	2.5	21.3	22.1	3.7%

3.3. Field application in Shuangdingshan Colliery

3.3.1. Scheme design

Water injection method was also applied in the –300 left-wing coal face in Shuangdingshan colliery. The thickness of the mining coal seam was 2.0 m and the expected height of the Fracturing zones has upper limit of $H_u = 16 \cdot M = 16 \times 2.0 = 32$ (m), lower limit of $H_l = 12 \cdot M = 12 \times 2.0 = 24$ (m) and the caved zone height of $H_c = 5 \cdot M = 5 \times 2.0 = 10.0$ (m). Boreholes for observation were drilled in the observation roadway. Data of boreholes are shown in Table 5, Fig. 11.

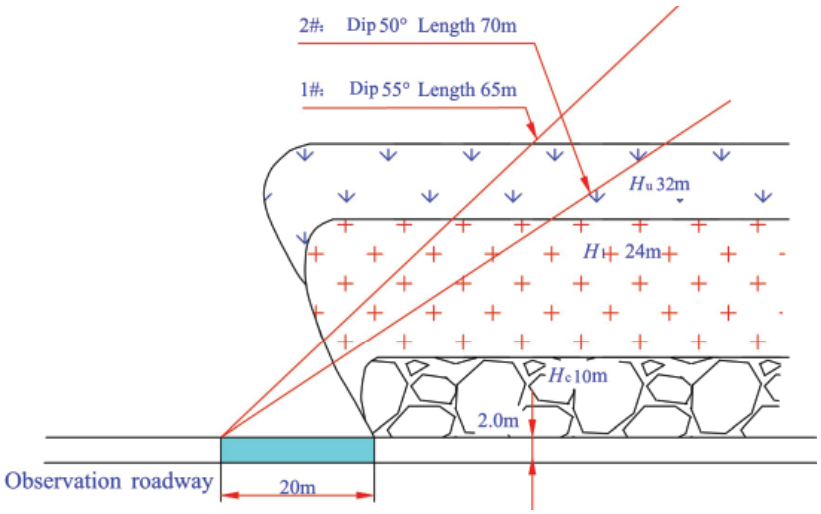

Fig. 11. Cross-sectional view of drilling layout in the –300 left-wing coal face

TABLE 5

Data of boreholes in the –300 left-wing coal face

Hole No.	Dip angle	Length (m)	Aperture (mm)
1	55°	65	ϕ89
2	50°	70	ϕ89

3.3.2. Results and analyses

According to the measured data, the seepage quantity and water outflow of 1# and 2# drillings are shown in Fig. 12.

1) Observed results of 1# drilling

The boreholes in the I drilling area was 30.88~40 m long and 25.3~32.8 m high. The seepage quantity was ranged from 2.24 to 5.85 L/min and less than 5 L/min in most cases. In addition, secondary cracks were not developed. Because of low seepage quantity, the FRACTURING ZONES was not formed in the area.

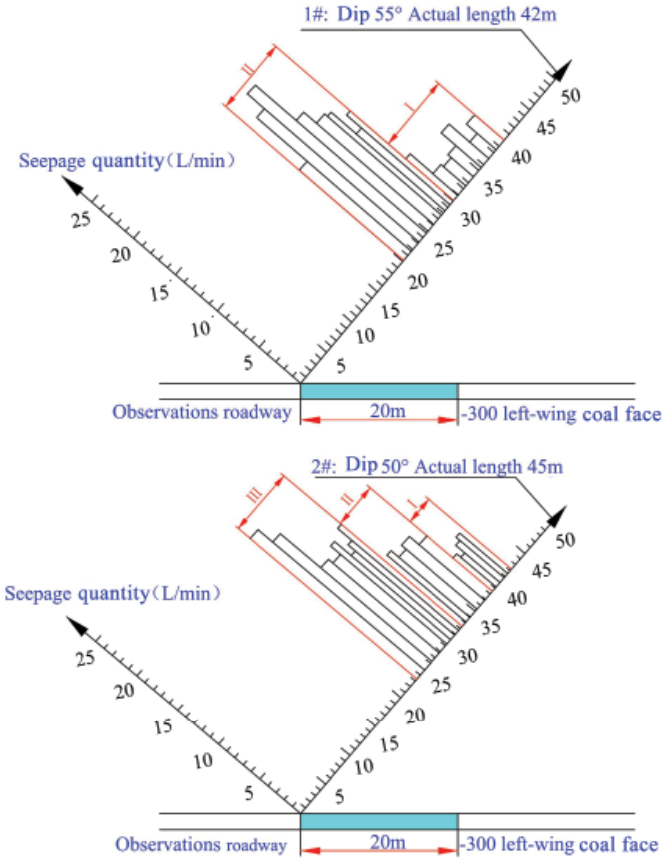

Fig. 12. Observed results of 1# and 2# drillings

The boreholes in the II drilling area was 21.76~30.12 m long and 17.8~24.7 m high. The seepage quantity was ranged from 10.74 to 20.45 L/min. Because of higher seepage quantity, the drilling penetrated the Fracturing zones, which was less affected by mining. In addition, secondary cracks were not developed. The rock showed high conductivity. When the vertical height of drillings reduced from 25.3 to 24.7 m, the seepage quantity increased from 5.85 to 12.35 L/min. The maximum height of the FRACTURING ZONES was about 24.7 m.

2) Observed results of 2# drilling

The boreholes in the I drilling area was 39.24~42.28 m long and 30~32.4 m high. The seepage quantity was ranged from 3.6 to 5.9 L/min and less than 2 L/min in most cases. In addition, secondary cracks were not developed. The I drilling area had strong impermeability and integrity, and was less affected by mining.

The boreholes in the II drilling area was 33.16~38.48 m long and 25.4~29.5 m high. The seepage quantity was ranged from 7.3 to 9.8 L/min. Taking the field test error into consideration, the actual seepage quantity was from 3 to 6 L/min. Pre-existing fractures were developed in this area and the Fracturing zones affected by mining was not in this area.

The boreholes in the III drilling area was 24.8~32.4 m long and 19.0~24.8 m high. The seepage quantity was ranged from 12.1 to 20.3 L/min. Considering the field test error, the actual seepage quantity was ranged from 9 to 18 L/min, and greater than 10 L/min in most cases. Therefore, drillings penetrated the Fracturing zones. Induced by mining, secondary cracks were developed and had a high conductivity. When the vertical height of drillings reduced from 25.4 to 24.8 m, the seepage quantity increased from 7.33 to 14.88 L/min. The maximum height of the Fracturing zones was about 24.8 m and determined by the 2# drilling.

3.3.3. Determination of the height of Fracturing zones

Table 6 lists the data of rock strata. It can be seen from Table 6, that from the coal face to the 4.06 m thickness conglomerate, the vertical height was 22.29 m, consistent with the 2# observational data. The vertical height from coal place to tuffaceous sandstone was 35.32 m, greater than the scope of measured results. In order to ensure production safety, the maximum observed result should be the height of Fracturing zones in the –300 left-wing coal face.

TABLE 6

Data of geological drilling in Shuangdingshan colliery

Lithology	Thickness /m	Cumulative thickness /m	Vertical height from coal place /m
Tuffaceous glutenite	36.12	356.90	101.59
Silty mudstone	30.15	387.05	65.47
Tuffaceous sandstone	13.03	400.08	35.32
Conglomerate	4.06	404.14	22.29
…	…	…	…
Argillaceous siltstone	3.27	431.24	6.05

Combining the rock strata and observed results of seepage quantity, the height of Fracturing zones in the -300 left-wing coal face was determined to be 24.8 m. Table 7 lists the measured and theoretical data of Shuangdingshan Colliery.

TABLE 7

Comparison between measured the height of the Fracturing zones with theoretically calculated value

Colliery	Mining thickness /m	Rock type	Strength coefficient (*f*) in fracture zone	The measured height of the Fracturing zones /m	The theoretical height of the Fracturing zones /m	Error
Shuangdingshan	2.0	Medium-hard	3.0	24.8	24.7	0.4%

From Tables 4 and 7, it is obvious that the measured the height of the Fracturing zones of Dongrong colliery was 21.3 m, the theoretical height of the Fracturing zones was 22.1 m and the error rate was 3.7%, which was in the permissible range of error. The measured height of the Fracturing zones in Shuangdingshan colliery was 24.8 m, the theoretical height of the Fracturing zones was 24.7 m and the error is 0.4%, also in the permissible range of error. In other words, the method is feasible and could be used to guide methane drainage.

4. Engineering application

4.1. Design and layout of high drilling methane drainage

The 7433 coal face of Kongzhuang colliery has a dip angle of the coal seam of 22~28° with average about 25°, thickness of 4.6 m, mining height of 2.4 m and bulk factor of 1.35. According to the empirical formula and Eq. 6, the distribution of overlying rock strata vertical three zones in the 7433 coal face of Kongzhuang colliery was determined and shown in Table 8. As shown, the scope of high drilling was 15.3~35.2 m. Three rows of high drilling were arranged in the test field, as shown in Figs 13 and 14. The height of upper drillings was controlled in the range of 28.5 to 35.2 m, the height of middle drillings in the range of 21.9 to 28.5 m, and the height of bottom drillings in the range of 15.3 to 21.9 m.

TABLE 8

Distribution of "vertical three zones" in the 7433 coal face

Three zones	Theoretical distribution (range from 7th seam roof) /m
Caved zone	0~15.3
Fracture zone	15.3~35.2
Continuous deformation zone	>35.2
The horizontal distance	16.0~20.1

The cross-sectional and top viewport of NO. 3 drill field are shown in Figs 13 and 14, respectively. The drilling diameter was extended to 108 mm when it (#1) was blocked. The total depth was extended to 22 m and completely blocked, with tube length of 20 m. The drilling diameter was extended to 108 mm when they (# 2 and # 3) were blocked. Their total depth was 10 m and completely blocked with tube length of 10 m. The shortest distance from the end of blocking to the 7433 tail gate was greater than 4.9 m, beyond the scope of roadway loose circle. The roof's angle of break was 61° and the average caved interval under the periodic variation of the roof surface pressures was 10 m. Thus, the stubble distance was ≥ 30 m.

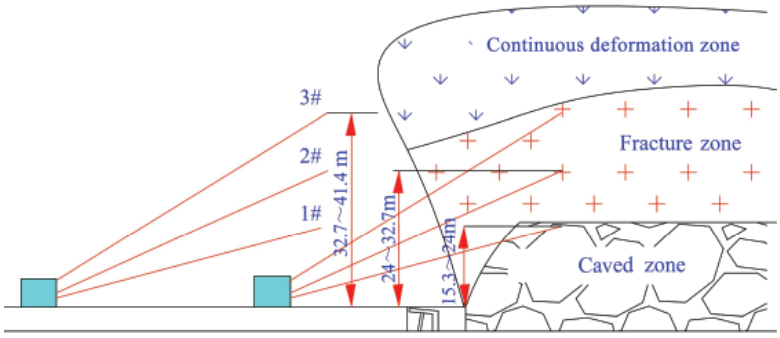

Fig. 13. Cross-sectional view of drilling

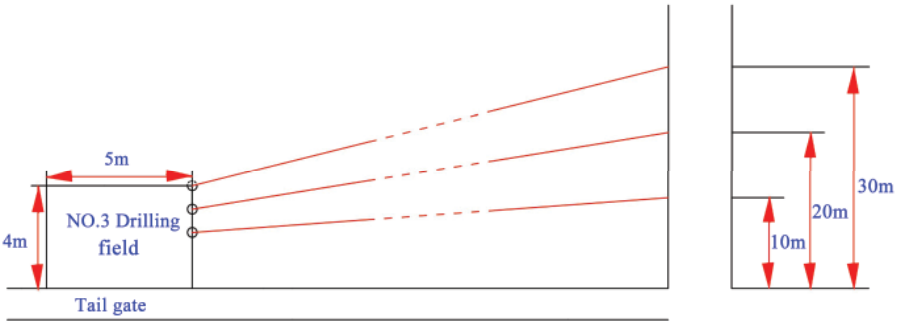

Fig. 14. Top viewport of drilling

4.2. Results and discussion

According to the above results, the HDMD in the 7433 coal face was designed and carried out. Based on the data collected from Oct. 15, 2012 to Oct. 30, 2012, including HDMD, buried pipe methane drainage, and ventilation air methane, we performed the following analyses.

1) Methane concentration in ventilation

The methane concentration under the conditions of ventilation was tested at night of each day. Fig. 15 shows the trend of methane concentration.

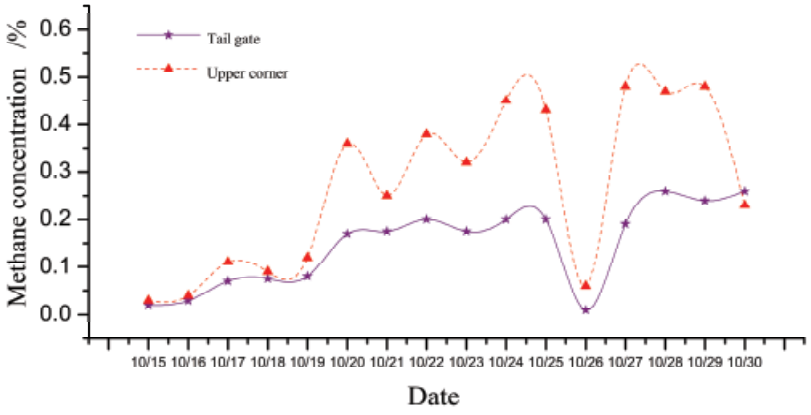

Fig. 15. Methane concentration changes with time in the conditions of ventilation air methane

2) High drilling methane drainage

During HDMD, the methane concentration reached 3~4.8% and the drainage quantity was 32~35 m^3/min. Thus, the pure volume of methane extraction per hour was 57~100 m^3. Fig. 16 shows the trend of methane concentration in Oct. 28, 2012 in the conditions of HDMD. Before drainage, methane concentrations in the upper corner and the tail gate reached 0.47% and 0.22%, respectively. From 8:00 to 9:00 am after starting HDMD, methane concentration decreased rap-

idly to 0.1% and 0.15% in the upper corner and the tail gate. Three hours later, it rose to 0.15% when the pump was stopped at 12:00.

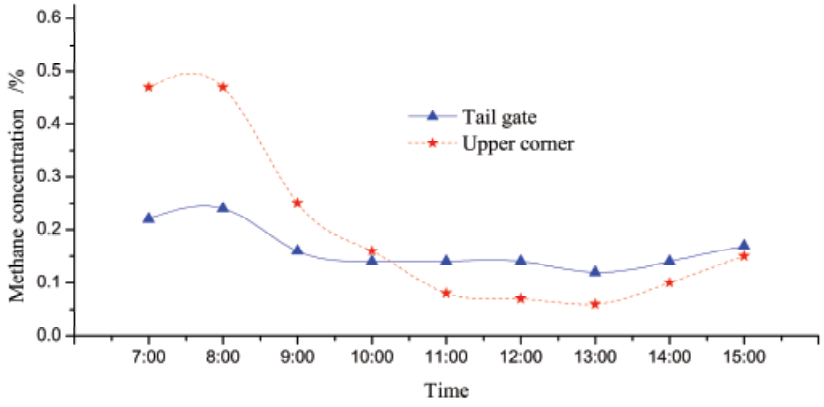

Fig. 16. Methane concentration changes with time in the conditions of HDMD on Oct 28

3) Buried pipe methane drainage

With buried pipe methane drainage, methane drainage concentration reached 0.18~0.32% and the drainage quantity was 90~95 m^3/min, i.e., the pure volume of methane extraction per hour was 10~18 m^3. Fig. 17 shows the trend of methane concentration in the conditions of buried pipe methane drainage on Oct. 19, 2012. Before drainage, methane concentration in both upper corner and tail gate were 0.47% and 0.22%, respectively. From 8:00 to 9:00 am after starting to extract methane, methane concentration decreased to 0.15% and 0.2% in the upper corner and tail gate, respectively. At 12:00 when pumping was stopped, the methane concentration rose rapidly.

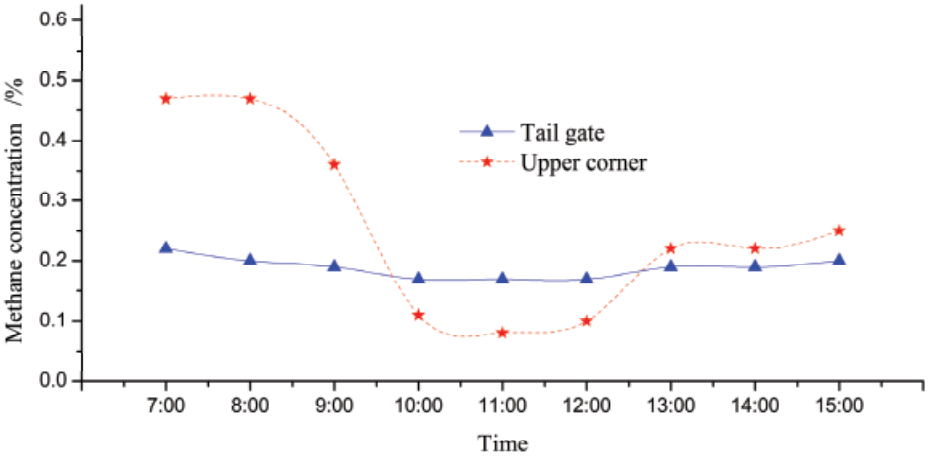

Fig. 17. Methane concentration changes with time in the conditions of buried pipe drainage on Oct. 29

Through statistical analysis of drainage quantity and methane concentrations on site, the pure volume of methane extraction per hour in HDMD was found to be 4 to10 times as much as that in buried pipe methane drainage. The drainage quantity in HDMD was 1/3 times as much as that in buried pipe methane drainage. Therefore, the air-leakage rate in gob was greatly reduced, which means that the application of HDMD can effectively reduce the occurrence of spontaneous combustion. Therefore, its advantage is obviously greater than that of buried pipe methane drainage.

Fig. 18 shows the comparison among the trends of methane concentration in the conditions of buried pipe methane drainage, HDMD and ventilation air methane. The pure average volume of methane extraction was 0.16 m^3/min in the conditions of buried pipe methane drainage and 4.60 m^3/min in the conditions of ventilation air methane, while the pure average volume was 60.6% of the total methane emissions in HDMD.

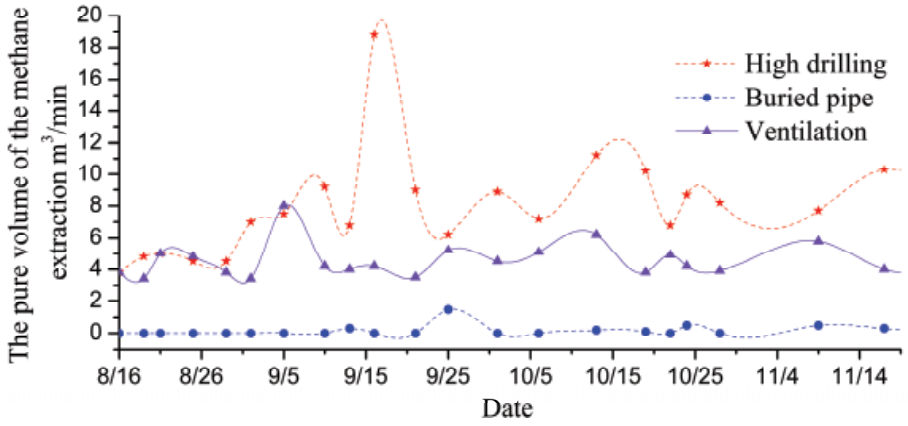

Fig. 18. Comparison among methane concentrations in different conditions at 7433 coal face

In four months of mining, the pure volume of methane extraction in HDMD was 32 m^3/min. The effect of methane drainage increased to 54.6%, the methane concentration in tail gate was controlled in the range of 0.17% to 0.32%, and the methane concentration in the upper corner was controlled in the range of 0.26% to 0.84%, all of which revealed that application of HDMD could improve production safety at the working place.

5. Conclusions

From the above mentioned researches on the water injection verified HDMD in the Fracturing zones, the following conclusions were reached.

1) The characteristics of Fracturing zones are similar to those of the AFZs, so the HDMD can be designed based on the distribution of Fracturing zones. According to the height of Fracturing zones obtained from the field observation and the formula of the deduced strata strain, assuming that two segments of arcs can be used to fit the inner and outer brim curves of the subsidence trough, the relationship between the Fracturing zones height and strength coefficient was found.

2) Comparison between the experimental observations and theoretical calculations was conducted by using the water injection and the geological drilling in Dongrong colliery and Shuangdingshan colliery. The results showed that the experimentally measured and theoretically calculated the height Fracturing zones of Dongrong colliery were 21.3 m and 22.1 m, respectively, with an error rate of 3.7%; while the corresponding values of Shuangdingshan colliery were 24.8 m and 24.7 m, respectively, with an error of 0.4%. Both of these errors were smaller than 5% and in the permissible range, indicating that the method is feasible and could be used to guide methane drainage.
3) Based on the application of the fitted relationship between Fracturing zones height and strength coefficient, combined with the empirical formula and the theory of strain, the scope of HDMD (15.3 to 35.2 m) was determined in the 7433 coal face of Kongzhuang colliery. According to the height of Fracturing zones, the project aiming at HDMD was implemented in Kongzhuang colliery and the methane drainage results were compared with those using buried pipe methane drainage, and ventilation air methane. The results showed that the pure volume of methane extraction per hour in HDMD was 4 to10 times as much as that in the buried pipe methane drainage, the drainage quantity in the HDMD was 1/3 times as much as that in the buried pipe methane drainage, the pure average volume of the methane extraction in the HDMD was 60.6% of the total methane emissions, the effect of methane drainage increased to 54.6%, the methane concentrations in both the tail gate and upper corner were controlled within regulation values. Thus, the problem of methane overrun was solved effectively.

Acknowledgement

The authors gratefully acknowledge each mine workers, for the technical support and the height of water flowing fracture zone measurements as well as for further interesting discussions. The authors would like to acknowledge the support of Scientific Research Foundation of State Key Lab. of Coal Mine Disaster Dynamics and Control (2011DA105287–FW201411), National Natural Science Foundation Project (51304128, 51304237), Shandong Provincial Natural Science Foundation, China (ZR2013EEQ015) and Specialized Research Fund for the Doctoral Program of Higher Education (20133718120013).

References

Abbas M., Ferri P.H., Mehdi Y.N., 2012. *Prediction of the height of destressed zone above the mined panel roof in longwall coal mining*. International Journal of Coal Geology, 98(1), 62-72.

Castro R., Trueman R., Halim A., 2007. *A study of isolated draw zones in block caving mines by means of a large 3D physical model*. International Journal of Rock Mechanics & Mining Sciences, 44(6), 860-870.

Chen J.H., Wang T., Zhou Y. et al., 2012. *Failure modes of the surface venthole casing during longwall coal extraction: A case study*. International Journal of Coal Geology, 90-91(1), 135-148.

Cheng J.Y., Feng L.W., Ji Y.L. et al., 2015. *A comprehensive methodology for predicting shield support hazards for a U.S. coal mine*. DYNA, 90(4), 442-450.

Dai H.Y., Lian X.G., Liu J.Y. et al., 2010. *Model study of deformation induced by fully mechanized caving below a thick loess layer*. International Journal of Rock Mechanics & Mining Sciences, 47(6), 1027-1033.

Flores R.M., 1998. *Coalbed methane: from hazard to resource*. International Journal of Coal Geology, 35(1-4), 3-26.

Frank H., Ting R., Naj A., 2013. *Evolution and application of in-seam drilling for gas drainage*. International Journal of Mining Science and Technology, 23(4), 543-553.

Gjetvaj G., Tadić M., 2014. *The effect of water hammer on pressure increases in pipelines protected by an air vessel*. Tehnički vjesnik, 21(3), 479-484.

Li B., Wei J., Li P., et al., 2014. *Nonlinear motion law of coalbed gas seepage under the combined effects of stress and temperature*. Journal of Power Technologies, 94(2): 106-113.

Liu L.C., Yuan P., Wang H.F., 2009. *Principle and engineering application of pressure relief gas drainage in low permeability outburst coal seam*. Mining Science and Technology, 19(3), 342-345.

Liu Y.W., Liu M.J., Wei J.P., 2011. *Regional outburst-prevention technique by gas pre-drainage based on large diameter boreholes along coal seams under deep mining*. Procedia Engineering, 26(1), 623-629.

Lu T.K., Yu H., Zhou, T.Y. et al., 2009. *Improvement of methane drainage in high gassy coal seam using water jet technique*. International Journal of Coal Geology, 79(1-2), 40-48.

Miao X.X., Cui X.M., Wang J.A., 2011. *The height of fractured water-conducting zone in undermined rock strata*. Engineering Geology, 120(1-4), 32-39.

Noack K., 1998. *Control of gas emissions in underground coal mines*. International Journal of Coal Geology, 35(1-4), 57-82.

Peng S.J., Xu J., Yin G.Z. et al., 2012. *Spatial-temporal evolution of gas migration pathways in coal during shear loading*. International Journal of Mining Science and Technology, 22(6), 769-773.

Perez C.T., Becerra J.M.C., de Dios G.J.J., 2013. *An efficient methodology for generating virtual environments in railway driving simulators*. DYNA, 2013, 88(4), 433-443.

Ren W.Z., Guo C.M., Peng Z.Q. et al., 2010. *Model experimental research on deformation and subsidence characteristics of ground and wall rock due to mining under thick overlying terrane*. International Journal of Rock Mechanics and Mining Sciences, 47(4), 614-624.

Sang S.X., Xu H.J., Fang L.C. et al., 2010. *Stress relief coalbed methane drainage by surface vertical wells in China*. International Journal of Coal Geology, 82(3-4), 196-203.

Singh M.M., Kendorski F.S., 1983. *Strata disturbance prediction for mining beneath surface water and waste impoundments*. Proc. 1st Conference on Ground Control in Mining, Uni. West Virginia, 20(1), 76-89.

Tokhmchi B., Memarian H., Rezaee, M., 2010. *Estimation of the fracture density in fracture zones using petrophysical logs*. Journal of Petroleum Science and Engineering, 72(1-2), 206-213.

Wang G., Sun L.L., Qu H.Y., 2014. *Numerical simulation on the partition of gas-rich region in overlying strata*. Journal of Engineering Science and Technology Review, 7(1), 154-158.

Wang H.F., Cheng Y.P., Wang L., 2012. *Regional gas drainage techniques in Chinese coal mines*. International Journal of Mining Science and Technology, 22(6), 873-878.

Xu Z.M., Sun Y.J., Dong Q.H. et al., 2010. *Predicting the height of water-flow fracture zone during coal mining under the Xiaolangdi reservoir*. Mining Science and Technology, 20(3), 434-438.

Zhai C., Yu X., Ni G.H., 2013. *Microscopic properties and sealing performance of new gas drainage drilling sealing material*. International Journal of Mining Science and Technology, 23(4), 475-480.

Zhang M.H., Wu S.Y., Wang Y.W., 2012. *Research and application of drainage parameters for gas accumulation zone in overlying strata of goaf area*. Safety Science, 50(4), 778-782.

Zhang S.T., Liu Y., 2012. *A simple and efficient way to detect the mining induced water-conducting fracture zone in overlying strata*. Energy Procedia, 16(1), 70-75.